ROYAL SOCIETY
OF CHEMISTRY

HIGHLIGHT

Check for updates

Crystal chemistry of dithienylethene photochromic switches†

Francoise M. Amombo Noa, iD *ab Joakim Andréasson iD b and Lars Öhrström iD *b

Diarylethene (DAE)-based photochromic molecules, *e.g.*, dithienylethenes, have emerged as versatile candidates for molecular switching over a very broad application range. Their popularity can be rationalized by the robust reversible photo-induced transformations, high thermal stability, excellent fatigue resistance, and reactivity in the solid state. This highlight emphasizes DAE performance in the solid-state. It explores, among other things, crystal structures, co-crystals, and metal–organic frameworks (MOFs). Although the DAE photochromic switches have been indispensable for research into light-responsive materials since their discovery in 1988, recent structural surveys and database studies reveal critical design challenges. Analysis of data in the Cambridge Structural Database, CSD, shows that dithienylethenes (DTEs) such as 1,2-bis[2-methylbenzo[*b*]thiophen-3-yl]-3,3,4,4,5,5-hexafluoro-1-cyclopentene, account for around 80% of crystal structures. Antiparallel geometry and short C···C distances govern photoactivity, but crystal packing frequently enforces non-reactive conformations, complicating rational design. Notable advances include metal–organic frameworks combining two distinct photoswitches (DAEs and spiropyrans), photoswitching between porous and non-porous phases, and rare single-crystal-to-single-crystal transformations in interpenetrated frameworks. Photomechanical crystals capable of face-dependent twisting and lifting weights 900× heavier than the crystal illustrate the potential of crystal engineering for actuators. These findings underscore both the opportunities and limitations in translating molecular photochromism into functional solid-state devices.

Diarylethene photochromism – since 1988

Photochromism is the reversible transformation between two isomers with distinct absorption spectra. Typically, one isomeric form absorbs in the visible region implying that it appears coloured, whereas the other absorbs mainly in the UV region, which is why it is often referred to as the colourless isomer. Systems that display no or very slow thermal isomerization reactions are referred to as P-type photoswitches, and these can only be isomerized by exposure to light of different wavelengths. Diarylethenes (DAE), such as the frequently used dithienylethenes, belong to this class of compounds, and their favourable photochromic properties have made them the switch of choice for many researchers aiming at photo-optical devices operating at both molecular and supramolecular magnitudes.[1–3]

a School of Health Sciences, Catholic University of Central Africa, P.O. Box 1110, Yaoundé, Cameroon
b Division of Chemistry and Biochemistry, Dept. of Chemistry and Chemical Engineering, Chalmers University of Technology, SE-41296 Gothenburg, Sweden. E-mail: mystere@chalmers.se, ohrstrom@chalmers.se
† To Professor Resnati, celebrating a career in fluorine and noncovalent chemistry on the occasion of his 70th birthday.

The discovery of the DAE photochromic systems implied a significant advance, as Irie and co-workers could show that with methyl-substituted heterocyclic rings these compounds "have no thermochromic property and the coloured form is stable even at elevated temperature".[4] Thus these systems could be cycled back and forth using light while being thermally stable in both the open and the closed form.

In the crystalline state, DAE photoswitches exhibit nearly unity (≈100%) photocyclization quantum yields because all open isomers are typically constrained in the antiparallel conformation, that is, the only conformation that can undergo ring-closure, whereas in solution the open isomers populate parallel and antiparallel forms equally. For photocycloreversion, several crystals show quantum yields similar to those in solution, but others display quantum yields 2–3 times higher due to restricted, non-relaxed conformations of the photogenerated closed isomers within the crystal lattice. Thus, crystallinity enhances the efficiency of both forward and backward photoisomerization when molecular packing enforces reactive conformations or limits structural relaxation.[5]

Since then, these versatile photoswitches have been suggested for potential applications across various fields, including chemistry, nanotechnology, and biology.[7–12] In here, we will exemplify the structural chemistry of the DAEs in the crystalline form, also emphasizing its supramolecular aspects.

Important properties of the diarylethenes

As indicated above, the photophysical assets of DAEs in solution as well as in solid state are high isomerization quantum yields for the colorization reaction, large differences in the maximum absorption wavelength between the two isomers, good resistance to photofatigue, and short response times.[10,12,13]

Moreover, the absence of thermal isomerization is important in many applications. Reported DAE derivatives exhibit half-lives up to hundreds of thousands of years at room temperature.[14,15] As for the fatigue resistance, that is, the ability to cycle between the two isomers repeatedly with no or little photodegradation, it is critical for practical applications and more than 14 000 cycles in solution and 30 000 cycles in the single crystalline phase have been reported.[16–18]

Although we will herein exclusively highlight systems triggered by photoisomerization, there are reports of alternative isomerization stimuli, like electrochemistry and pH.[19]

Synthesis of diarylethenes

Invariably the diarylethenes are initially prepared in the open form. The preparation of diarylethenes is not trivial though, and their large variety means an extensive organic synthesis tool book has been used,[20] preventing an exhaustive overview. As an illustrating example, we chose to highlight a facile synthetic procedure for perhydrocyclopentenes and perfluorocyclopentenes (such as **2o**, see Fig. 1) reported by Feringa and co-authors in 2003.[21] The procedure can be carried out on a large scale with inexpensive starting materials.[22]

Photochromic properties

The perhydro- and perfluorocyclopentene derivatives exhibit equivalent photochromic behaviour, with high isomerization quantum yields (>0.6 to 1 for the colorization reaction) and photoconversion efficiencies (0.85–1).[23]

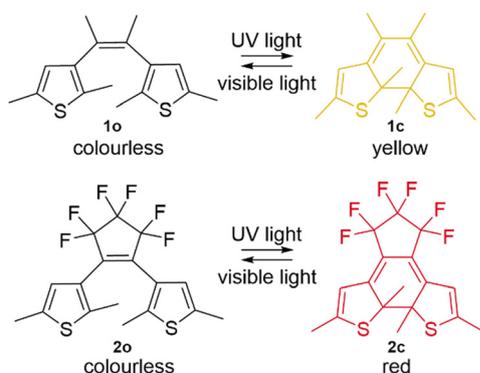The main differences between these two classes lie in their photochemical and thermal stability. Some perhydrocyclopentene derivatives undergo nearly quantitative photochemical isomerization unlike their perfluoro counterparts.[1–3] Despite this, both types can undergo multiple switching cycles without significant photodecomposition with thermal interconversion half-lives exceeding 3 hours at 100 °C. This makes perhydrocyclopentenes excellent alternatives in most applications, while perfluorocyclopentenes might be better suited for data storage applications requiring high fatigue resistance and thermal stability.

The photo-induced cyclization of diarylethenes

Photo-induced cyclization of DAE derivatives occurs when the open form is exposed to UV light, undergoing a conrotatory cyclization to form a closed-ring isomer. This closed form is coloured and has distinct absorption properties compared to the open form.[11,15] Several factors influence the cyclization of DAE molecules, including the nature of aryl groups, the central ethene bridge, and additional substituents that affect the reaction rate.[11,24–26]

Thermal stability

Both the open and closed forms of DAE derivatives exhibit exceptional thermal stability, with half-lives extending to hundreds of thousands of years at room temperature.[14,15] Many DAE derivatives, including those containing thiophenes, benzothiophenes, furans, and perfluoro-cyclopentene, can retain their coloured (closed) form for extended periods, even at elevated temperatures (e.g., 100 °C), before reverting to the thermodynamically stable, colourless open form in the dark.[11,15,24,27,28]

Thermal stability can be governed by the choice of substituents. For example, research by Li and Zeng showed that incorporating spirobifluorene groups significantly improved the thermal stability of both open and closed forms. The spirobifluorene open derivative had a 59 °C higher thermal stability judged from a 5% weight loss limit during thermogravimetric analysis (TGA) and the closed form showed significantly lower conversion back to the open form
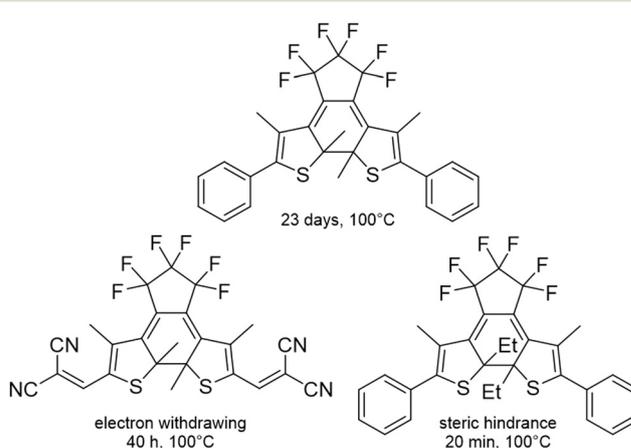

Fig. 1 Two diarylethene (DAE) photochromic systems with **o** and **c** denoting open and closed forms. Top: Compound **1** from the first report in 1988,[4] and bottom: 1,2-bis(2,5-dimethyl-3-thienyl) perfluorocyclopentenes **2**.[6]

Fig. 2 Examples of thermal stability of DAE closed forms.[30]

in solution.[29] Fig. 2 illustrates the thermal stability of selected DAE derivatives.[30]

The importance of thermal stability lies in its relevance to applications such as optical data storage, photoswitchable molecular devices, and other technologies where maintaining the coloured state over time is crucial.[24,27] It is important to note that the thermal stability of the closed isomer is not correlated with the photocycloreversion quantum yield. This is because the potential energy surface of the ground state differs from that of the excited states, which control the photocycloreversion quantum yield.[11]

Fatigue resistance

Fatigue resistance is a key property of DAE-based molecules, allowing them to undergo numerous photochromic cycles without significant degradation. Some DAE compounds can repeat cyclization – cycloreversion more than 14 000 times in solution and 30 000 cycles in the single crystalline phase.[16–18]

Fatigue resistance can be affected by several factors, including chemical structure,[27,31] host–guest interactions,[32] polymeric matrices[33] and excitation conditions.[31] It can be improved by optimizing the chemical structure of DAEs with specific substituents to enhance stability and reduce byproduct formation during photoisomerization. For instance, Chung and co-authors[34] have shown a strategic substitution of functional groups at specific reaction sites, using molecular switches for high performance polymer field-effect transistors (FETs). Their system displays switching ratios of 4405 and excellent electrical fatigue resistance over 100 switching cycles. Other strategies to improve fatigue resistance include: controlling the surrounding environment at which the experiment is conducted,[33,34] substitution with 3,5-bis(trifluoromethyl)phenyl or 3,5-bis(pentafluorosulfanyl) phenyl groups[32,35] and using supramolecular complexes.[31,36]

The solid-state

To date, several thousand DAE derivatives have been prepared, and more than a hundred articles are published each year as judged by the Web of Science database. Although most of these reports concern properties in the solution phase, some recent advances emphasize solid-state properties.

For example, morphological control of patterning by sublimation has recently been achieved using 1,2-bis(2,5-dimethyl-3-thienyl)perfluorocyclopentenes, **2o** (Fig. 1, right),[37] and photosalient[38] and bio-mimetic functions were recently reviewed.[39]

The Cambridge Structural Database (CSD)[40] contained 1349 unique DAE structures in 2023, either in open- or closed ring forms.[41] Notably, only the open-ring isomers with antiparallel aryl group geometry[25] and a reactive carbon separation of approximately 4.20 Å are photoactive.[42,43]

These CSD structures can be grouped into dithienylethenes (~80%), dibenzothienylethenes (~8%), and asymmetric DAEs (~7%), with dipyrrolylethenes and difurylethenes in equal parts making up the rest (Fig. 3).[41]
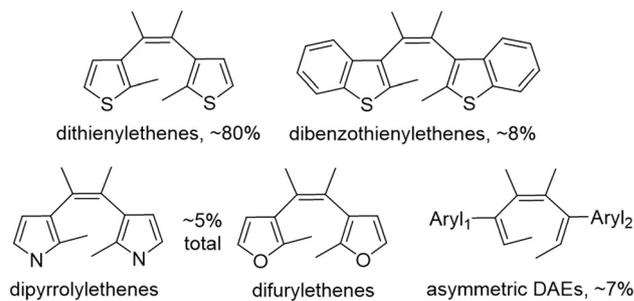

Fig. 3 Classification of the 1349 unique DAE structures either in open (shown) or closed (not shown) ring forms in the Cambridge Structural Database.[41]

Crystal growth

DAE derivatives can be crystallized using standard techniques with the crystallization process influenced by specific DAE derivatives and solvent choice.[44] Common methods include solubility-based crystallization, solvent selection, slow cooling, vapor diffusion and sublimation.

In solubility-based crystallization, the compounds are dissolved in a suitable solvent at elevated temperatures to form a saturated solution which is then cooled to allow crystal formation. The solvent must dissolve the compounds well at high temperatures but poorly at lower temperatures. Solvent polarity and intermolecular interactions are key factors that affect the choice of solvent.[44,45] The slow cooling method promotes the formation of larger, well-defined crystals. Other techniques such as vapor diffusion and sublimation are also employed, especially for volatile compounds.[37]

Substituents and functional groups affect solubility and crystallization behavior.[44,46] Another major factor is temperature. It plays a crucial role in solubility and crystal deformation. Solvent selection is also important to achieving successful crystallisation.[44] There are also impurities, which are to be removed through filtration of the solution before cooling. This helps discard any insoluble impurities that hinder crystal growth. These considerations are essential for obtaining high-quality DAE crystals for structural and functional studies.

Basic solid-state and molecular parameters, the size of open and closed diarylethenes

The first DAE crystal structure was obtained for 1,2-bis(3,5-dimethyl-3-thienyl)perfluorocyclopentene **3o**[47,48] and one of the first determinations of structures of both open and closed forms was for the 2,5-dimethyl-3thienyl derivative, **2o** and **2c**.[6] While the open form has more flexibility in crystal packing, the closed form appears more compact as the ring closure makes the two aromatic parts come closer and the molecule becomes flatter, see Fig. 4. The effect on molecular volume on **2** as judged by the unit cells (none of the structures contain any significant voids) is that the closed form is 1% smaller than the open form at room temperature, a difference that is
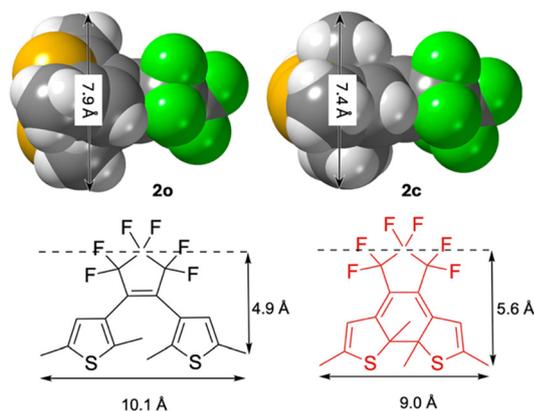
Fig. 4 Basic dimensions and dimension changes of diarylethenes using data from one of the first single crystal X-ray diffraction determinations of the structures of both open and closed forms of a diarylethene.[6] These dimension changes are consistent with the closed form being smaller, 1–2.5% judging by the unit cell changes.

enhanced at 123 K to 2.5%, both cells shrinking as the temperature drops.

This difference is consistent with the size measurements given in Fig. 4. If an orthogonal parallelepiped is assumed with these metrics to approximate the size, then the shrinking of **2** from open to closed will be 4.6%. However, under the assumption that 56% of the molecule retains its geometry (14 out of 25 heavy atoms do not move significantly) then 2.6% is a more reasonable estimate.

It should be noted that with larger substituents specific crystal packing may lead to reverse effects, so that both shrinking and expansion of the unit cells are possible upon irradiation of the open form.

Structural requirements for photochemical activity

There are also two structural requirements on the open form of the diarylethene for photoisomerization to occur:

Antiparallel conformation of the methyl groups is the photoactive form. This allows the two reactive carbon atoms to approach each other and undergo conrotatory photocyclization, forming the closed-ring isomer. This conformation has C_2 symmetry, which is symmetry-allowed for the electrocyclic reaction under the Woodward–Hoffmann rules.[49] (The parallel conformation can be seen in Fig. 15 for **23o**.)

The C⋯C distance of the reacting carbon atoms. The photocyclization yield has been shown to drop dramatically to almost zero for distances larger than 4.2 Å.[50]

Single-crystal-to-single-crystal (SCSC) transformations. Single-crystal-to-single-crystal (SCSC) transformations of DAEs are possible upon light irradiation. This means that the crystal retains its integrity while undergoing a structural change, which is essential for applications in optical memory and actuators. The ability to undergo SCSC transformations depends on crystal packing and the availability of free volume to accommodate molecular motion. The first reported transformation of this kind for a DAE derivative is usually

credited to Kobatake *et al.* in 1999.[6] The SCSC transformations may be accompanied by a visible change in crystal size and morphology, see further below in the section Photodeformable crystals.

Surveys of structural DAE data in the CSD

The rational design of photoactive DAE-based crystalline solids is complicated by the conformational flexibility caused by the free rotation of the aryl groups in the open isomeric form. While the chemical influence of substituent groups can be judged by the solution behaviour, the effect of the conformational flexibility on the solid-state structures is less obvious to access. In principle these data can be found in the now more than 1350 CSD structures, but the geometric analysis is not straightforward.

One parameter is the C⋯C distance, as described above. Can it be rationally designed to be shorter than the critical 4.2 Å threshold for SCSC transformations?

Recently Öhrström *et al.*, in connection with reporting new closed and open structures of iodobenzene thiophene 1,1-dioxide DAEs, analysed CSD data of perfluorocyclopent-1-ene-diaryl derivatives.[51] Based on the critical C⋯C distances and the ethylene-aryl torsion angle they found a majority of structures, >85%, having a C⋯C distance of around 3.5 Å, and lower mean torsion angles around 40°, whereas a smaller maximum around 4.2 Å in the angle *vs.* distance plot roughly correlated with torsion angles around 90°. Larger torsion angles may be related to steric crowding, so this was vaguely suggested as a reason for this correlation.

However, as subsequently pointed out by Benedict and co-workers in 2024, use of a mean torsion angle does not capture all the complexity of these compounds. In their more comprehensive study of 1349 DAE structures, they corroborate the 4.2 Å secondary maxima but noted that the majority of these structures have the parallel conformation, and the photocyclization is thus forbidden by the Woodward–Hoffmann rules. But there is a significant fraction of the photoactive antiparallel conformations as well.[41]

In an earlier experimental study from 2023, Benedict and co-workers embedded the diphenylene DAE **4** (Fig. 5), that on its own was found in two polymorphs, in 17 different crystalline solids such as co-crystals, coordination polymers,
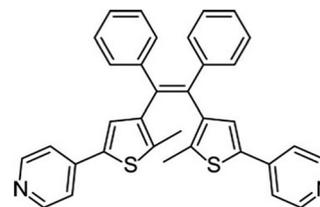

Fig. 5 The DAE (*Z*)-1,2-bis(2-methyl-5-(pyridin-4-yl)thiophen-3-yl)-1,2-diphenylethene **4o** embedded in 19 independent crystalline materials by Benedict and co-workers where only 2 of the crystal structures suggested photochemical activity of **4**, thus with C⋯C less than 4.2 Å and an antiparallel conformation of the methyl groups.

and MOFs.[52] Notably, compound **4** has a slightly different conformation in each of these crystal structures, and, more significantly, the C···C distances vary greatly from 3.73 Å to 5.36 Å with only two of them being photoactive.

Though a limited sample, this study does suggest that the potential energy surface of individual DAE molecules is so flat that weak intermolecular interactions easily push the DAE molecule out of its individual energy minima.

The three studies together suggest, in the words of Benedict and co-workers, to which we completely agree, that "The large width of the distribution of geometries with respect to the torsion angle (approximately 30–160°) is consistent with molecules adopting structures within the lattice that likely do not correspond to energetic minima of isolated molecules".[41]

We also agree with Benedict and co-workers that there may be a bias in the data reported to the CSD.[41] One may suspect that successfully prepared photoswitching materials will more often have their structures reported than more conventional non-photochromic compounds, and that the chemical and structural landscape painted by the available date thus is somewhat tinted. This highlights the need to report all crystal structures.

Potential applications of DAEs

DAEs have a wide range of applications across various fields, including molecular switching,[44,53–55] optical data storage,[14,44,53] memory,[11,53,56] bioimaging,[36,53,57] controlling molecular properties,[25] fluorescence switching,[36,58–60] light controlled self-assembly,[14,53] catalysis,[36] molecular logic gates,[61] photomechanical devices,[44,53] and photoswitchable ionic liquids.[44] The relevance to some of these in the crystalline state is discussed below.

Photoswitching. Photoswitching is most often implemented in solution and will therefore only be highlighted by one example herein. Switching between open and closed forms of the DAE derivative Dasy **4** (Fig. 6) was demonstrated by Andréasson and co-authors,[62] where the open form (Dasy(o)) absorbs in the UV region with a peak at 351 nm in aqueous media. Upon exposure to UV light at 365 nm, isomerization occurs, yielding nearly 100% of the closed form (Dasy(c)) at the photostationary state (PSS), with a corresponding isomerization quantum yield of 0.44. Dasy(c) absorbs in the visible region with a maximum at 644 nm. When exposed to visible light at 523 nm, Dasy(c) reverts to 100% Dasy(o) with an isomerization quantum yield of 0.0033. Notably, Dasy(c) is non-fluorescent, whereas Dasy(o) exhibits fluorescence emission at around 511 nm in aqueous solution as shown in Fig. 6b.

Photodeformable crystals. Photodeformable crystals depend on SCSC transformations as discussed above. This implies that such DAE crystals undergo macroscopic deformation due to volume changes associated with isomerization.[14] The first example is generally believed to be Kobatake *et al.* who in 2007 reported photoinduced bending of rod-like crystals of **6o** and also reversible shrinkage and
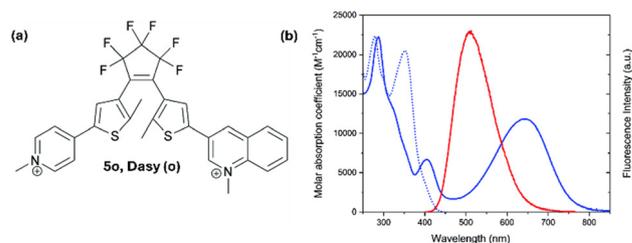
Fig. 6 (a) The DAE cation Dasy by Andréasson and co-authors.[62] (b) absorption and emission spectra of Dasy in aqueous solution. Dotted blue line: Dasy(o) absorption. Solid blue line: Dasy(c) absorption. Red line: Dasy(o) emission. Dasy(c) has no detectable emission.

expansion of the rectangular plate-shaped single crystal, consistent with our brief discussion of molecular volumes.[63]

Photodeformable crystals by crystal engineering

Mixed DAE co-crystals can also be grown, and rod-shaped hybrid crystals of **7o** and **8o** were used to convert light to mechanical energy, lifting a weight almost 1000 times heavier than the crystal, the effect being ascribed to a large Youngs modulus.[64] Co-crystals may also be obtained with other non-photoactive components, *i.e.* the DAE 1,2-bis(2-methyl-5-(1-naphthyl)-3-thienyl)perfluorocyclopentene **9o** with perfluoronaphthalene **10**, as shown in Fig. 7 and 8.[65]
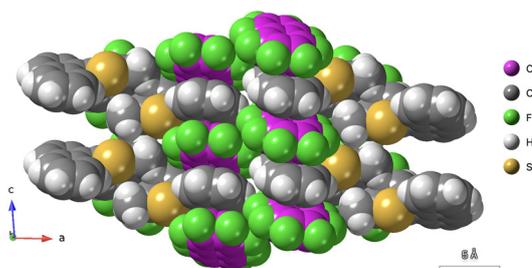
Fig. 7 Co-crystal of 1,2-bis(2-methyl-5-(1-naphthyl)-3-thienyl) perfluorocyclopentene **9o** with perfluoronaphthalene **10**, CSD code CIXBAN02.[65]
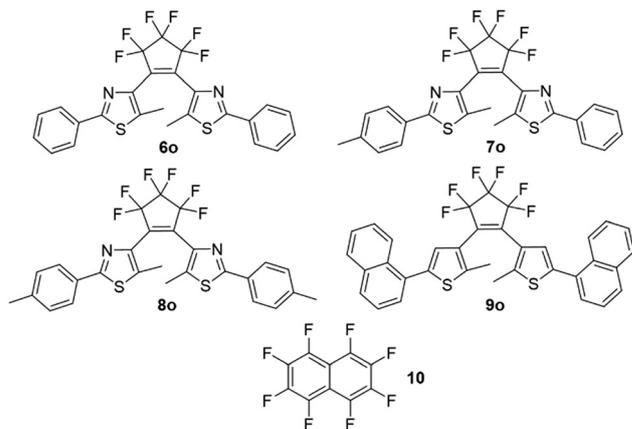
Fig. 8 Photodeformable DAE crystals were grown from **6o**,[14] and co-crystals of **7o** and **8o**,[64] and also from co-crystals of **9o** and **10**.[65]
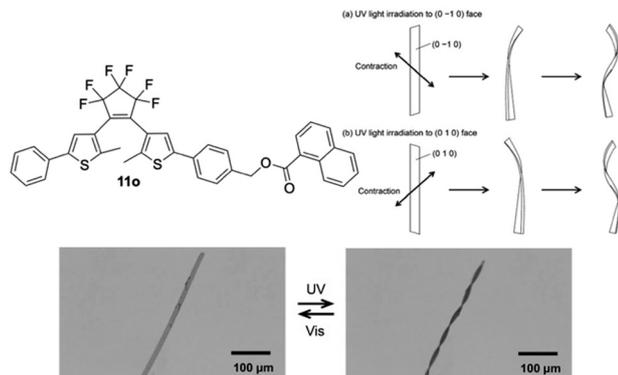
Fig. 9 Photodeformable DAE crystals were grown from **11o** and, as depicted schematically (top) and experimentally (bottom), showed face dependent twisting when irradiated with UV-light.[66] Reproduced with permission from ref. 65, copyright © 2013 WILEY-VCH Verlag GmbH & Co. KGaA, Weinheim.

Another feature due to crystal engineering was shown by Kitagawa *et al.* for **11o**. Different crystal faces showed different responses to UV-light, thus when the (0 −1 0) face was irradiated a right-handed twist was obtained, and *vice-versa* for irradiation of the (0 1 0) face, see Fig. 9.[66]

The DAEs can also be incorporated into inorganic structures giving photodeformable crystals. Kajiya and coworkers added polyhedral oligomeric silsesquioxane (POSS) linked by amide bonds to a DAE benzothiophene (Fig. 3) suggesting enhanced thermal stability because of the POSS units ([RSiO$_{1.5}$]$_8$, R = *i*Bu, Ph).[67]

Later, Dong *et al.* used commercially available aluminium oxide (AAO), a porous template with pore diameters of 200 nm, to grow nanocrystals in the internal channels of AAO using a DAE both contracting and expanding.[68]

DAEs in metal–organic frameworks

Moving from crystal engineering to coordination polymers (CPs) and metal–organic frameworks (MOFs),[69] we note that the first examples, a 1D Cu(I) coordination polymer, used the nitrile substituted DAE **12o**[70] but subsequent studies have mainly been using either the carboxylate derivatives **13o** and **14o**, or the pyridines **15o** or **16o**, see Fig. 10. For an overview, we can see that to date in the CSD the MOF subset contains 18 structures with **13o** or **14o**, and 22 with **15o** or **16o**.

For reference we also show the fairly common V-shaped MOF linker oba[71] that has similar angular metrics to **14o** and **15o**. The oba linker has an average angle of 125° between the carboxylate carbons and the bridging oxygen (measured on 520 structures in the Cambridge Structural Database),[71] whereas the core of **15o** and **16o** has an average angle of 112° between the carboxylate carbons and the ethylene bridge centroid (based on 34 structures in the CSD). The three closed forms of **14o** found in the CSD have an angle of 108°, which is going to be fairly invariant as the structure is very rigid.
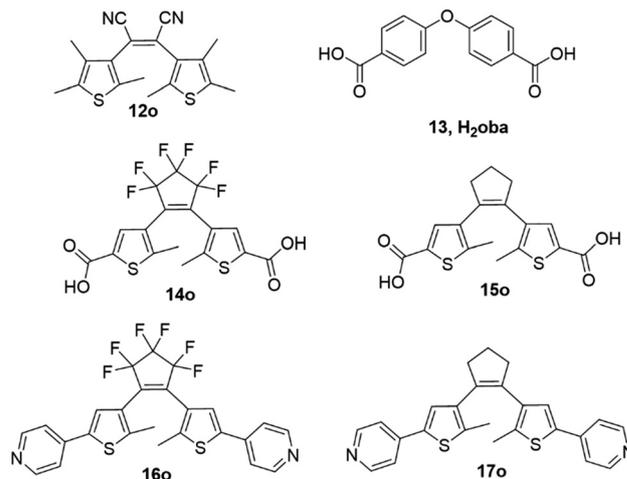

Fig. 10 The first examples of a DAE coordination polymer (CP) used **12o** but many later examples of both CPs and metal–organic frameworks (MOFs) were made with **14–17**, a 1D Cu(I) coordination polymer used the nitrile substituted DAE **12o**.[70]

These angles are fairly unimportant for 1D coordination polymers, but, as has been shown for oba MOFs, these V-shaped linkers do not fit into the blueprint of existing network topologies. This is due to the less than perfect mapping of their propagation vectors onto high symmetry nets,[71] and the same will be true for DAEs **13–17**.

In general, we find that there is a scarcity of MOFs exhibiting genuine single crystal to single crystal transformations (SCSC) with resolved open and closed structures.

Two aspects may be especially important. Molecular DAEs are often dense structures with close packed molecules but with weak intermolecular interactions between them. This leaves little space to move in, but weaker forces to overcome to rearrange the molecules. MOFs on the other hand have strong network bonds that might be quite rigid, but normally considerable space for movement due to the porosity. This suggests SCSC transformations to be more likely in systems close to soft and dynamic MOFs.[72]

Han *et al.* reported a set of 1D CPs with Co(II) and **14o** including solid-state photoisomerization, but could not obtain an X-ray structure on the closed form.[73] Later Morimoto *et al.* made a {Mn(II/III)$_4$} based single-molecule magnet (SMM) with the same linker in both open and closed forms that showed reversible photochromic behaviour.[74] Both crystal forms were obtained, though by independent synthesis, not by photoconversion.

Ln(III) 2D frameworks have also been made using **14o**, *i.e.* [Dy$_2$(**14o**)$_3$(dmso)$_3$(MeOH)]·10MeOH that showed photo-controlled SMM behaviour.[75] Shustova and co-workers made 2D Cu(II) and Zn(II) MOFs out of both **15o** and **17o** and showed the possibility of tuning metal oxidation states by switching between the two linker photoisomers.[76] Also in this case, there is no crystal structure of the closed form MOF for neither of the DAE linkers.

Employing Zn(II), the carboxylate linker H₂bpdc, biphenyl-4,4′-dicarboxylic acid, and **17o** Luo *et al.* obtained a fivefold interpenetrating **dia** net showing photocontrolled CO_2 capture and release, but again did not present the crystal structure of the closed form.[77] (For topology symbols and network analysis‡ see for example O'Keeffe and co-workers,[78] Bonneau *et al.*,[79] and Öhrström.[80]).

However, in 2017 Kitagawa and co-workers could determine the structure of both open and closed forms of the two-fold interpenetrated **pcu** MOF [Zn₂(bdc)₂(**16o**)]·dmf (bdc = benzene-1,4-dicarboxylare). The original open form was irradiated at 30 min giving [Zn₂(bdc)₂(**16c**) through a SCSC transformation.[81]

Also, in 2017 Barbour and co-workers incorporated conformational flexibility into the dicarboxylic acid co-ligands by using the bent oba linker **13**, and the ethyl variety of **16o**, **16o-Et** forming [Zn₂(**16o-Et**)(oba)₂] and [Zn₂(**16c-Et**)(oba)₂]. This gave a double interpenetrated **pcu** network, see Fig. 11, with notable deformation going from open [Zn₂(**16o-Et**)(oba)₂], (DMOF30, orange) to closed form [Zn₂(**16c-Et**)(oba)₂] (iDMOF30, blue). The photoconversion reduced the cell volume, and it was noted that this also implied leaving behind negligible guest-accessible pockets of only 20 Å³ each.[82]

More recently Shustova and co-workers prepared the first example of a double photoswitching MOF by incorporating DAE **17o** with spiropyran **19c** and the tetratopic carboxylate linker **18** dbtd. This gave various ratios of [Zn₂(**17o**)ₓ(**19c**)ᵧ(dbtd)], $x + y = 1$ in a paddle wheel based 4- and 6-connected MOF forming the **fsc**-net based on octahedra and squares, see Fig. 12. The preparations were carried out by preparing [Zn₂(**17o**)(dbtd)] and then adding the second photochromic unit by solvent-assisted ligand exchange (SALE). [Cu₂(**17o**)(dbtd)] was also prepared from [Zn₂(**17o**)(dbtd)] by metal ion metathesis and crystal structures of both these MOFs were obtained. They noted that using heat as the stimulus allows for selective activation of the spiropyran **19c** *versus* DAE **17o**.[83]
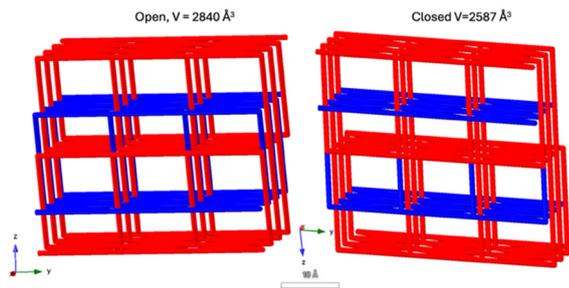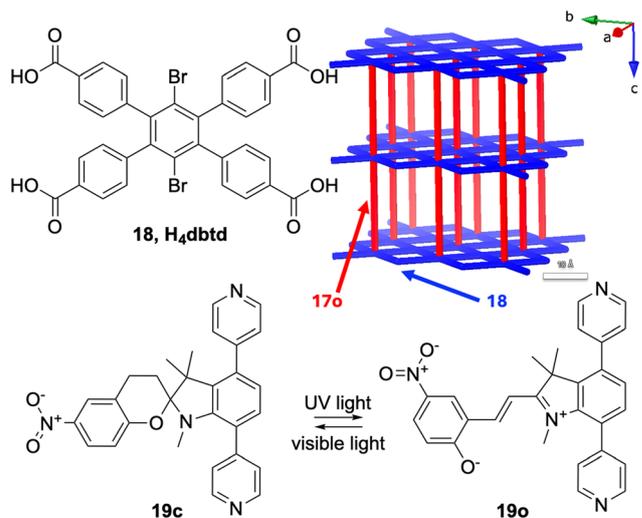

Fig. 12 Double photoswitching by incorporating the DAE **17o** with the spiropyran **18c** and the tetratopic carboxylate linker **18** dbtd giving various ratios of [Zn₂(**17o**)ₓ(**19c**)ᵧ(dbtd)], $x + y = 1$ in a padel wheel based MOF[83] forming the 4- and 6 connected **fsc**-net shown in the upper right corner, drawn from the crystal structure of [Zn₂(**17o**)(dbtd)].

Also in 2023, Zaworotko and co-workers reported DAE MOFs based on H₂dpt, 2,5-diphenylbenzene-1,4-dicarboxylic acid **20**, and H₂fdpt=5-fluoro-diphenylbenzene-1,4-dicarboxylic acid **21** giving [Cd(**16o**)(dpt)₂], LMA-1-α, and [Cd(**16o**)(fdpt)₂], described by the 8-connected **hex**-net, see Fig. 13. LMA-1-α can go through two subsequent phase transitions reducing the cell volume to form LMA-1-β and then LMA-1-γ1 which are all colourless. Then LMA-1-γ1 can go through a SCSC photoconversion to finally give the dark blue LMA-1-γ1-UV. Notably, the activated MOF LMA-1-γ2, depending on the extent of irradiation, can reversibly reduce its loading capacity by 30–55% by transforming to LMA-1-γ2-UV.[84]

This study accentuates both the importance of recognizing multiple phase transformations occurring due to different solvents and activation procedures, but also the difference the substitution of two hydrogen atoms for two fluorine atoms has on the sorption properties.

Coordination polymers

In relation to the MOFs, we note a dense coordination polymer reported in 2025, [Feᴵᴵ(**16o**)₂{Ag(CN)₂}₂{Ag(CN)}₂] that features both spin transition of the Fe(II) centre and DAE photochromism. However, in this triply interpenetrated 3,6-net no SCSC conversion could be achieved as the photoconversion in the sold state is low. Despite this observation, subtle magnetic switching was observed with UV irradiation.[85] The 3- and 6-connected net in this material seems not to have been described before, see SI.§

Fig. 11 The two interpenetrated **pcu**-nets in [Zn₂(**16o-Et**)(oba)₂] (DMOF30) and [Zn₂(**16c-Et**)(oba)₂] (iDMOF30). The change in volume is significant upon ring closure leaving behind negligible guest-accessible pockets of only 20 Å³ each.[82]

---

‡ If not present in the original articles, network topology was determined using SYSTRE[93] and TopCryst.[94]

§ Details of the new 3,6-net in [Feᴵᴵ(**16o**)₂{Ag(CN)₂}₂{Ag(CN)}₂] is given in the SI. This net is binodal with 4 kinds of edges and has point symbol {5³}₂{4⁴·5⁵·6²·7⁴·8}.
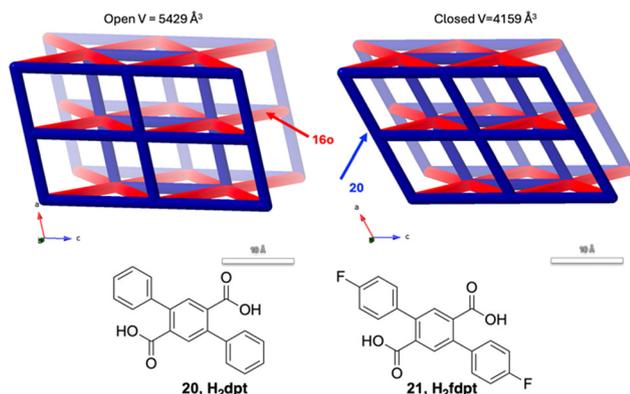
Fig. 13 [Cd(**16o**)(dpt)$_2$] LMA-1-α and [Cd(**16c**)(dpt))$_2$] LMA-1-γ1-UV both described by the 8-connected **hex**-net. LMA-1-α can go through two subsequent phase transitions reducing the cell volume to form LMA-1-β and then LMA-1-γ1 which are all colourless. Then LMA-1-γ1 can go through a SCSC photoconversion to finally give the dark blue LMA-1-γ1-UV.[84] The DAE based network links (red) shrink from 20.2 Å to 18.1 Å going from the open to the closed form.

Fig. 14 Two DAEs were shown to exhibit optical waveguide properties. Note: **23o** contains two photoactive DAEs groups.

Fig. 15 The parallel conformation of the two thiophene rings (emphasised in black to the right) makes **23o** unavailable to induce the photocyclization reaction in the single crystalline phase. The head-to-tail packing mode of **23o** was suggested as responsible for the waveguide properties.

Optical data storage

Due to their photochromic properties, DAEs are also excellent candidates for optical data storage. Photon mode optical memories utilize these changes in photophysical properties for data storage.[59]

High density storage is achieved using DAEs thanks to their reversible photoisomerization, high fatigue resistance and thermal stability. Zhang and co-authors highlighted three main functional materials for optical data storage, with DAEs standing out due to their ability to switch reversibly and clean between isomers upon UV/visible irradiation.[86] This makes them suitable for molecular scale digital storage.[87] 3D optical data storage is also possible by incorporating DAEs into layered media, enabling data writing through multiphoton excitation or localized optical breakdown.[88–90] For example, DAE derivatives embedded in polymers have demonstrated read-write-erase capabilities, proving their suitability for write-once-read-many (WORM) systems.

Optical waveguide properties of DTE

DTE derivatives have been shown to exhibit optical waveguide properties since 1994. Optical waveguides are confining and directing light by total refractive-index contrast, allowing light to propagate over long distances with low loss. In this report dibenzothienyl **22o** (20%) in a polyethylene matrix was shown to exhibit refractive index changes depending on the concentration of **22c**.[91]

In contrast, the novel biphotochromic fluorescent switch **23o** (**N-2F**) (Fig. 14 and 15), which shows excellent optical waveguide properties in the single crystalline state, displays a parallel conformation of the two thiophene rings, which makes **23o** unavailable to induce the photocyclization reaction in the single crystalline phase.[92] Instead, the optical waveguiding properties were attri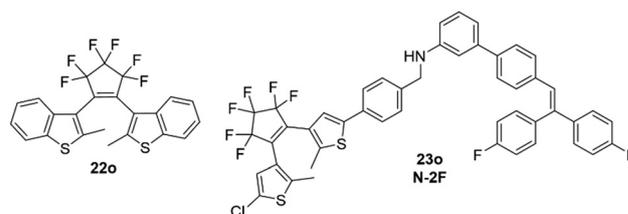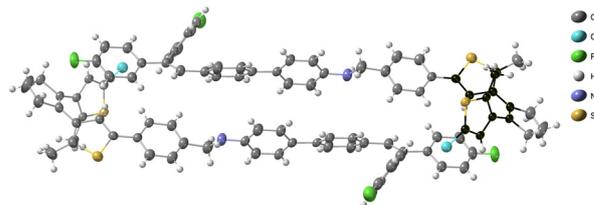buted to the molecule **23o** being arranged in a typical head-to-tail mode (Fig. 15), making the molecular packing effectively avoiding π–π interactions.

Conclusions

Diarylethene-based photoswitches represent a cornerstone in the development of photoresponsive materials, offering a unique combination of bi-stability, rapid switching, and long-term durability. Their ability to undergo reversible photoisomerization with high quantum yields and minimal degradation enables a wide array of potential applications, from molecular electronics and optical memory to bioimaging and logic gate systems. Advances in synthesis and crystallization have facilitated the design of DAEs with tailored properties, while structural studies have deepened our understanding of their solid-state behaviour.

However, it is also clear from this brief survey that the potential energy surface of individual DAE molecules is so flat that weak intermolecular interactions easily push the DAE molecule out of its individual energy minima. This frequently means rotating the substituents on the critical carbon atoms out of the photoactive antiparallel conformation and out of the optimal C···C distance for effective photoisomerization. This means that the optimization of solid-state devices based on DAE containing materials is a much more demanding task than optimizing DAE properties in solution.

While SCSC transformations are frequently observed in molecular solids, the number of examples, where a DAE MOF, or coordination polymer in general, undergoes such a phase change and both crystals structures have been determined, is still low.

Conflicts of interest

There are no conflicts to declare.

Data availability

Acknowledgements

Notes and references

1 M. Irie, in *Molecular Switches*, 2001, pp. 37–62, DOI: 10.1002/3527600329.ch2.

2 T. Mrozek, A. Ajayaghosh and J. Daub, in *Molecular Switches*, 2001, pp. 63–106, DOI: 10.1002/3527600329.ch3.

3 Y. Yokoyama, in *Molecular Switches*, 2001, pp. 107–121, DOI: 10.1002/3527600329.ch4.

4 M. Irie and M. Mohri, *J. Org. Chem.*, 1988, **53**, 803–808.

5 M. Irie, T. Fulcaminato, K. Matsuda and S. Kobatake, *Chem. Rev.*, 2014, **114**, 12174–12277.

6 S. Kobatake, T. Yamada, K. Uchida, N. Kato and M. Irie, *J. Am. Chem. Soc.*, 1999, **121**, 2380–2386.

7 S. H. Kawai, S. L. Gilat and J.-M. Lehn, *Eur. J. Org. Chem.*, 1999, **1999**, 2359–2366.

8 B. M. Neilson and C. W. Bielawski, *ACS Catal.*, 2013, **3**, 1874–1885.

9 R. Göstl, A. Senf and S. Hecht, *Chem. Soc. Rev.*, 2014, **43**, 1982–1996.

10 M. Irie, *Chem. Rev.*, 2000, **100**, 1685–1716.

11 M. Irie, T. Fukaminato, K. Matsuda and S. Kobatake, *Chem. Rev.*, 2014, **114**, 12174–12277.

12 V. Balzani, A. Credi and M. Venturi, Bistable and Multistable Systems, in *Molecular devices and machines: concepts and perspectives for the nanoworld*, 2008.

13 V. Balzani, A. Credi and M. Venturi, in *Molecular Devices and Machines*, 2008, pp. 171–207, DOI: 10.1002/9783527621682.ch7.

14 C. Huang, R. Huang, S. Zhang, H. Sun, H. Wang, B. Du, Y. Xiao, T. Yu and W. Huang, *Research*, 2021, 102736.

15 M. Irie, *Proc. Jpn. Acad., Ser. B*, 2010, **86**, 472–483.

16 H. Jean-Ruel, M. Gao, M. A. Kochman, C. Lu, L. C. Liu, R. R. Cooney, C. A. Morrison and R. J. D. Miller, *J. Phys. Chem. B*, 2013, **117**, 15894–15902.

17 R. J. D. Miller, *Science*, 2014, **343**, 1108–1116.

18 M. Hanazawa, R. Sumiya, Y. Horikawa and M. Irie, *J. Chem. Soc., Chem. Commun.*, 1992, 206–207, DOI: 10.1039/C39920000206.

19 Q. Ai, K. Lan, L. Li, Z. Liu and X. Hu, *Adv. Sci.*, 2024, **11**, 2410524.

20 V. Z. Shirinian, D. V. Lonshakov, A. G. Lvov and M. M. Krayushkin, *Russ. Chem. Rev.*, 2013, **82**, 511–537.

21 L. N. Lucas, J. J. D. d. Jong, J. H. v. Esch, R. M. Kellogg and B. L. Feringa, *Eur. J. Org. Chem.*, 2003, **2003**, 155–166.

22 H. Tian and S. Yang, *Chem. Soc. Rev.*, 2004, **33**, 85–97.

23 J. J. D. d. Jong, L. N. Lucas, R. Hania, A. Pugzlys, R. M. Kellogg, Ben L. Feringa, K. Duppen and J. H. v. Esch, *Eur. J. Org. Chem.*, 2003, **2003**, 1887–1893.

24 R. Li, T. Ou, L. Wen, Y. Yan, W. Li, X. Qin and S. Wang, *Molecules*, 2024, **29**, 5202.

25 K. Matsuda and M. Irie, *J. Photochem. Photobiol., C*, 2004, **5**, 169–182.

26 J. C. Micheau, C. Coudret, O. I. Kobeleva, V. A. Barachevsky, V. N. Yarovenko, S. N. Ivanov, B. V. Lichitsky and M. M. Krayushkin, *Dyes Pigm.*, 2014, **106**, 32–38.

27 J. C.-H. Chan, W. H. Lam and V. W.-W. Yam, *J. Am. Chem. Soc.*, 2014, **136**, 16994–16997.

28 D. Chen, Z. Wang and H. Zhang, *J. Mol. Struct.: THEOCHEM*, 2008, **859**, 11–17.

29 C. Li and H. Zeng, *J. Heterocyclic Chem.*, 2016, **53**, 1706–1714.

30 D. Kitagawa, K. Sasaki and S. Kobatake, *Bull. Chem. Soc. Jpn.*, 2011, **84**, 141–147.

31 G. Pariani, M. Quintavalla, L. Colella, L. Oggioni, R. Castagna, F. Ortica, C. Bertarelli and A. Bianco, *J. Phys. Chem. C*, 2017, **121**, 23592–23598.

32 R. Miyamoto, D. Kitagawa and S. Kobatake, *Bull. Chem. Soc. Jpn.*, 2022, **95**, 639–645.

33 E. Samoylova, W. Dallari, M. Allione, F. Pignatelli, L. Marini, R. Cingolani, A. Diaspro and A. Athanassiou, *Mater. Sci. Eng., B*, 2013, **178**, 730–735.

34 S. Z. Hassan, J. Song, S. H. Yu and D. S. Chung, *Chem. Mater.*, 2021, **33**, 7546–7557.

35 M. Herder, B. M. Schmidt, L. Grubert, M. Pätzel, J. Schwarz and S. Hecht, *J. Am. Chem. Soc.*, 2015, **137**, 2738–2747.

36 S. K. Bag, A. Pal, S. Jana and A. Thakur, *Chem. – Asian J.*, 2024, **19**, e202400238.

37 M. Isobe, D. Kitagawa and S. Kobatake, *Small Methods*, 2025, **9**, 2401545.

38 P. Naumov, S. C. Sahoo, B. A. Zakharov and E. V. Boldyreva, *Angew. Chem., Int. Ed.*, 2013, **52**, 9990–9995.

39 R. Nishimura, S. Yokojima and K. Uchida, in *Advances in Organic Crystal Chemistry: Comprehensive Reviews 2025 on Crystal Functions*, ed. S. Kobatake and H. Uekusa, Springer Nature Singapore, Singapore, 2025, pp. 63–85, DOI: 10.1007/978-981-96-4479-7_4.

40 C. F. Macrae, I. J. Bruno, J. A. Chisholm, P. R. Edgington, P. McCabe, E. Pidcock, L. Rodriguez-Monge, R. Taylor, J. van de Streek and P. A. Wood, *J. Appl. Crystallogr.*, 2008, **41**, 466–470.

41 X. Zhang, T. B. Mitchell and J. B. Benedict, *Cryst. Growth Des.*, 2024, **24**, 6284–6291.

42 S. Kobatake, K. Uchida, E. Tsuchida and M. Irie, *Chem. Commun.*, 2002, 2804–2805, DOI: 10.1039/B208419H.

43 L. Öhrström, J. Andréasson, H. Li and F. M. Amombo Noa, *Cryst. Growth Des.*, 2024, **24**, 923–931.

44 M. R. C. Soromenho, C. A. M. Afonso and J. M. S. S. Esperança, *Int. J. Mol. Sci.*, 2023, **24**, 3533.

45 L. H. Nicoud and A. S. Myerson, in *Handbook of Industrial Crystallization*, ed. A. S. Myerson, D. Erdemir and A. Y. Lee, Cambridge University Press, Cambridge, 3rd edn, 2019, pp. 115–135, DOI: 10.1017/9781139026949.004.

46 D. G. Patel, M. Boggio-Pasqua, T. B. Mitchell, I. M. Walton, W. R. Quigley and F. A. Novak, *Molecules*, 2020, **25**, 2630.

47 M. Irie, K. Uchida, T. Eriguchi and H. Tsuzuki, *Chem. Lett.*, 1995, 899.

48 T. Yamada, S. Kobatake and M. Irie, *Bull. Chem. Soc. Jpn.*, 2002, **75**, 167–173.

49 R. B. Woodward and R. Hoffmann, *J. Am. Chem. Soc.*, 1965, **87**, 395–397.

50 S. Kobatake, K. Uchida, E. Tsuchida and M. Irie, *Chem. Commun.*, 2002, 2804–2805, DOI: 10.1039/B208419H.

51 L. Öhrström, J. Andréasson, H. Li and F. M. Amombo Noa, *Cryst. Growth Des.*, 2024, **24**, 923–931.

52 T. B. Mitchell, X. Zhang, R. T. Jerozal, Y.-S. Chen, S. Wang and J. B. Benedict, *IUCrJ*, 2023, **10**, 694–699.

53 Z. Li, X. Zeng, C. Gao, J. Song, F. He, T. He, H. Guo and J. Yin, *Coord. Chem. Rev.*, 2023, **497**, 215451.

54 V. Balzani, *Photochem. Photobiol. Sci.*, 2003, **2**, 459–476.

55 M. Irie, in *Diarylethene Molecular Photoswitches: Concepts and Functionalities*, 2021, pp. 1–240, ISBN: 978-3-527-34640-0.

56 J. Yang, Q. Zou, X. Chen, Y. Li, C. Zhao, T. Weng, B. Wu, L. Zhu, D. Wang and Z. Xin, *Dyes Pigm.*, 2021, **191**, 109361.

57 K.-X. Qin, Y.-S. Su, M.-Q. Zhu and C. Li, *ChemBioChem*, 2024, **25**, e202400326.

58 T. Fukaminato, S. Ishida and R. Métivier, *NPG Asia Mater.*, 2018, **10**, 859–881.

59 C. Yun, J. You, J. Kim, J. Huh and E. Kim, *J. Photochem. Photobiol., C*, 2009, **10**, 111–129.

60 M. Aydemir, G. Haykir, H. Selvitopi, O. C. Yildirim, M. E. Arslan, B. Abay and F. Turksoy, *J. Mater. Chem. B*, 2023, **11**, 4287–4295.

61 X. Ma, M. Lu, X. Wang, S. Cui and S. Pu, *Dyes Pigm.*, 2023, **211**, 111094.

62 G. Naren, W. Larsson, C. Benitez-Martin, S. Li, E. Pérez-Inestrosa, B. Albinsson and J. Andréasson, *Chem. Sci.*, 2021, **12**, 7073–7078.

63 S. Kobatake, S. Takami, H. Muto, T. Ishikawa and M. Irie, *Nature*, 2007, **446**, 778–781.

64 F. Terao, M. Morimoto and M. Irie, *Angew. Chem., Int. Ed.*, 2012, **51**, 901–904.

65 M. Morimoto and M. Irie, *J. Am. Chem. Soc.*, 2010, **132**, 14172–14178.

66 D. Kitagawa, H. Nishi and S. Kobatake, *Angew. Chem., Int. Ed.*, 2013, **52**, 9320–9322.

67 R. Kajiya, S. Sakakibara, H. Ikawa, K. Higashiguchi, K. Matsuda, H. Wada, K. Kuroda and A. Shimojima, *Chem. Mater.*, 2019, **31**, 9372–9378.

68 X. Dong, T. Guo, D. Kitagawa, S. Kobatake, P. Palffy-Muhoray and C. J. Bardeen, *Adv. Funct. Mater.*, 2020, **30**, 1902396.

69 S. R. Batten, N. R. Champness, X. M. Chen, J. Garcia-Martinez, S. Kitagawa, L. Öhrström, M. O'Keeffe, M. P. Suh and J. Reedijk, *Pure Appl. Chem.*, 2013, **85**, 1715–1724.

70 M. Munakata, L. P. Wu, T. Kuroda-Sowa, M. Maekawa, Y. Suenaga and K. Furuichi, *J. Am. Chem. Soc.*, 1996, **118**, 3305–3306.

71 C. L. F. Dazem, N. Ruser, E. Svensson Grape, A. K. Inge, D. M. Proserpio, N. Stock and L. Öhrström, *Dalton Trans.*, 2025, **54**, 5659–5663.

72 S. Krause, N. Hosono and S. Kitagawa, *Angew. Chem., Int. Ed.*, 2020, **59**, 15325–15341.

73 J. Han, M. Maekawa, Y. Suenaga, H. Ebisu, A. Nabei, T. Kuroda-Sowa and M. Munakata, *Inorg. Chem.*, 2007, **46**, 3313–3321.

74 M. Morimoto, H. Miyasaka, M. Yamashita and M. Irie, *J. Am. Chem. Soc.*, 2009, **131**, 9823–9835.

75 D. Pinkowicz, M. Ren, L.-M. Zheng, S. Sato, M. Hasegawa, M. Morimoto, M. Irie, B. K. Breedlove, G. Cosquer, K. Katoh and M. Yamashita, *Chem. – Eur. J.*, 2014, **20**, 12502–12513.

76 C. R. Martin, K. C. Park, G. A. Leith, J. Yu, A. Mathur, G. R. Wilson, G. B. Gange, E. L. Barth, R. T. Ly, O. M. Manley, K. L. Forrester, S. G. Karakalos, M. D. Smith, T. M. Makris, A. K. Vannucci, D. V. Peryshkov and N. B. Shustova, *J. Am. Chem. Soc.*, 2022, **144**, 4457–4468.

77 F. Luo, C. B. Fan, M. B. Luo, X. L. Wu, Y. Zhu, S. Z. Pu, W.-Y. Xu and G.-C. Guo, *Angew. Chem., Int. Ed.*, 2014, **53**, 9298–9301.

78 N. W. Ockwig, O. Delagado-Friedrichs, M. O'Keeffe and O. M. Yaghi, *J. Am. Chem. Soc.*, 2005, **38**, 176–182.

79 C. Bonneau, M. O'Keeffe, D. M. Proserpio, V. A. Blatov, S. R. Batten, S. A. Bourne, M. S. Lah, J.-G. Eon, S. T. Hyde, S. B. Wiggin and L. Öhrström, *Cryst. Growth Des.*, 2018, **18**, 3411–3418.

80 L. Öhrström, *Crystals*, 2015, **5**, 154.

81 Y. Zheng, H. Sato, P. Wu, H. J. Jeon, R. Matsuda and S. Kitagawa, *Nat. Commun.*, 2017, **8**, 100.

82 V. I. Nikolayenko, S. A. Herbert and L. J. Barbour, *Chem. Commun.*, 2017, **53**, 11142–11145.

83 G. R. Wilson, K. C. Park, G. C. Thaggard, C. R. Martin, A. R. Hill, J. Haimerl, J. Lim, B. K. P. Maldeni Kankanamalage, B. J. Yarbrough, K. L. Forrester, R. A. Fischer, P. J. Pellechia, M. D. Smith, S. Garashchuk and N. B. Shustova, *Angew. Chem., Int. Ed.*, 2023, **62**, e202308715.

84 D. C. Castell, V. I. Nikolayenko, D. Sensharma, K. Koupepidou, K. A. Forrest, C. J. Solanilla-Salinas, B. Space, L. J. Barbour and M. J. Zaworotko, *Angew. Chem., Int. Ed.*, 2023, **62**, e202219039.

85 A.-Q. Jian, J.-C. Liu, D. Li, Y.-Q. Qi, S.-G. Wu and M.-L. Tong, *Inorg. Chem. Front.*, 2025, **12**, 8492–8502.

86 D. Dai, Y. Zhang, S. Yang, W. Kong, J. Yang and J. Zhang, *Molecules*, 2024, **29**, 254.

87 A. Fihey, A. Perrier, W. R. Browne and D. Jacquemin, *Chem. Soc. Rev.*, 2015, **44**, 3719–3759.

88 W. Dallari, M. Scotto, M. Allione, E. Samoylova, F. Pignatelli, R. Cingolani, A. Athanassiou and A. Diaspro, *Microelectron. Eng.*, 2011, **88**, 3466–3469.

89 S. Pu, H. Tang, B. Chen, J. Xu and W. Huang, *Mater. Lett.*, 2006, **60**, 3553–3557.

90 H. Hu, J. Pei, D. Xu, G. Qi, H. Hu, F. Zhang and X. Liu, *Opt. Mater.*, 2006, **28**, 904–908.

91 N. T. Norihisa Tanio and M. I. Masahiro Irie, *Jpn. J. Appl. Phys.*, 1994, **33**, 1550.

92 M. Luo, J. Zhao, Y. Liu, L. Jiang, S. Wang and Z. Chi, *Adv. Opt. Mater.*, 2022, **10**, 2201195.

93 O. Delgado-Friedrichs, S. T. Hyde, M. O'Keeffe and O. M. Yaghi, *Struct. Chem.*, 2017, **28**, 39–44.

94 A. P. Shevchenko, A. A. Shabalin, I. Y. Karpukhin and V. A. Blatov, *Sci. Technol. Adv. Mater.: Methods*, 2022, **2**, 250–265.